Reconstruction from Truncated Projections in Cone-beam CT using an Efficient 1D Filtering

Yan Xia[a,b], Andreas Maier[a], Hannes G. Hofmann[a], Frank Dennerlein[c], Kerstin Mueller[a,b], and Joachim Hornegger[a,b]

[a]Pattern Recognition Lab (LME), Friedrich-Alexander-University Erlangen-Nuremberg, Erlangen, Germany;
[b]Graduate School in Advanced Optical Technologies (SAOT), Friedrich-Alexander-University Erlangen-Nuremberg, Erlangen, Germany;
[c]Healthcare Sector, Siemens AG, Erlangen, Germany

ABSTRACT

In X-ray imaging, a reduction of the field of view (FOV) is proportional to a reduction in radiation dose. The resulting truncation, however, is incompatible with conventional tomographic reconstruction algorithms. This problem has been studied extensively. Very recently, a novel method for region of interest (ROI) reconstruction from truncated projections with neither the use of prior knowledge nor explicit extrapolation has been published, named Approximated Truncation Robust Algorithm for Computed Tomography (ATRACT). It is based on a decomposition of the standard ramp filter into a 2D Laplace filtering (local operation) and a 2D Radon-based filtering step (non-local operation).

The 2D Radon-based filtering that involves many interpolations complicates the filtering procedure in ATRACT, which essentially limits its practicality. In this paper, an optimization for this shortcoming is presented. That is to apply ATRACT in one dimension, which implies that we decompose the standard ramp filter into the 1D Laplace filter and a 1D convolution-based filter. The convolution kernel was determined numerically by computing the 1D impulse response of the standard ramp filtering coupled with the second order anti-derivative operation. The proposed algorithm was evaluated by using a reconstruction benchmark test, a real phantom and a clinical data set in terms of spatial resolution, computational efficiency as well as robustness of correction quality.

The evaluation outcomes were encouraging. The proposed algorithm showed improvement in computational performance with respect to the 2D ATRACT algorithm and furthermore maintained reconstructions of high accuracy in presence of data truncation.

Keywords: Image reconstruction, truncation correction, dose reduction, cone-beam CT, region of interest

1. INTRODUCTION

Although CT technology reached its maturation in the past decade, some novel technology trends still have evolved and revitalized this field. Amongst these major tendencies, reduction in radiation dose without compromising the image quality has increased its utility in the diagnostic and therapeutic applications. In some clinical applications and workflows (e.g. examination of deployed stents or coils after the intervention, cochlear implants, and needle biopsy) only a small portion of the whole patient may be diagnostically of interest, which enables the idea of utilizing X-ray beam collimation to laterally and axially block radiation during CT examination. The resulting truncation, however, introduces artificial high frequencies in the vicinity of truncation edges, prohibiting accurate analysis in the reconstructions.

So far many practical algorithms specially concerning the ROI reconstruction have been proposed and established. Some methods[1–7] can provide exact or high accurate reconstruction for ROI imaging. But they require either a prior information in the object, or additional radiation dose, scans for determining patient outline. Some are even computational intensive and complicated, which may essentially delay the interventional procedures. Another category of ROI reconstruction is based on estimating the missing data using an extrapolation procedure, such as symmetric mirroring of projection

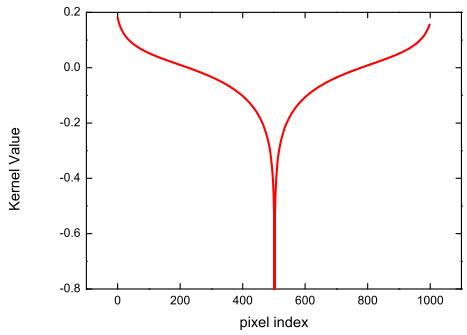

Figure 1. Illustration of 1D numerical convolution kernel.

images,[8] water cylinder/ellipse extrapolation,[9,10] square root extrapolation,[11] or optimization-based extrapolation.[12] However, these methods are based on heuristic assumptions that may not always accurately approximate the objects outside the ROI.

Very recently, a novel method (ATRACT) has been suggested for ROI reconstruction from truncated projections with neither the use of prior knowledge nor explicit extrapolation.[13] In this method, the parallel-beam Radon transform and inverse Radon transform are performed in each projection, which is computationally expensive. To increase the computational efficiency, an optimization was suggested that Radon-based filtering can be substituted by a 2D convolution.[14,15] Still the 2D filtering process is slower than the standard row-wise ramp filter. It is therefore our goal to simplify the filtering procedure of ATRACT without compromising its robustness with respect to truncated data.

2. MATERIALS AND METHODS

2.1 FDK Algorithm

Most contemporary X-ray C-arm CT systems employ the Feldkamp, Davis, and Kress (FDK) algorithm[16] due to its simplicity and efficiency. It typically consists of three steps: 1) Cosine and Parker weighting of the projections, 2) 1D row-wise ramp filtering of the pre-weighted projections, 3) 3D cone-beam backprojection.

2.2 2D ATRACT

Intuitively, the idea behind ATRACT is to adopt the FDK algorithm by decomposing the 1D ramp filter operation into two successive 2D filter steps. Therefore, the ATRACT algorithm can be written as follows: 1) Cosine and Parker weighting of the projections, 2) 2D Laplace filtering of the pre-weighted projections, 3) 2D convolution-based filtering of the second derivative projections, 4) 3D cone-beam backprojection.

2.3 1D ATRACT

The 1D ATRACT algorithm is also given by a modification of standard ramp filter in the FDK algorithm. It consists of the following steps: 1) Cosine and Parker weighting of the projections, 2) 1D Laplace filtering of the pre-weighted projections, 3) 1D residual filtering of the second derivative projections, 4) 3D cone-beam backprojection. The 1D residual filter kernel can be obtained by numerically computing the impulse response of the standard ramp filter coupled with the 1D inverse Laplace operation. The plot of the 1D numerical kernel is shown in Figure 1. Note that the kernel has some non-negative components which seem to be incorrect. In the practical implementation, we need to filter out these values to ensure accuracy of the reconstruction.

Figure 2 shows the comparison of the 1D ATRACT filtering and the ramp filtering in the case of truncated projections. We can see that high frequency artifacts are introduced by the ramp filter in the truncated projection. This will considerably degrade image quality in the reconstruction. In contrast, 1D ATRACT successfully excludes artificial high frequencies (removal of high spikes) after the Laplace filtering step, and subsequently performs the residual filtering to obtain the desired filtered projections. Moreover, because of the reduced computational complexity and less padding required in 1D FFTs, 1D ATRACT is expected to deliver an improvement in computational performance compared to 2D ATRACT.

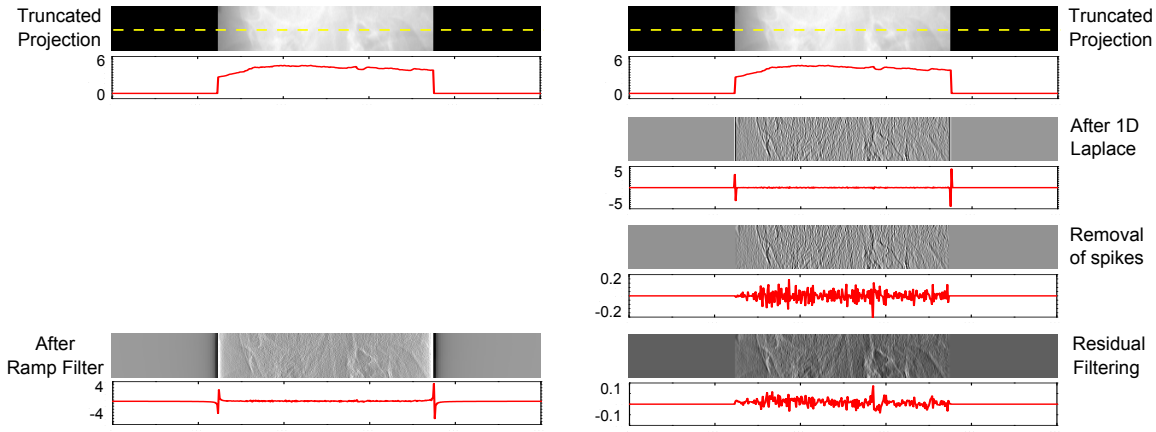

Figure 2. Comparison of the different filtering process by ramp filter and 1D ATRACT filter. Left column: Ramp filtering of a truncated projection. Right column: 1D ATRACT filtering of the same truncated projection.

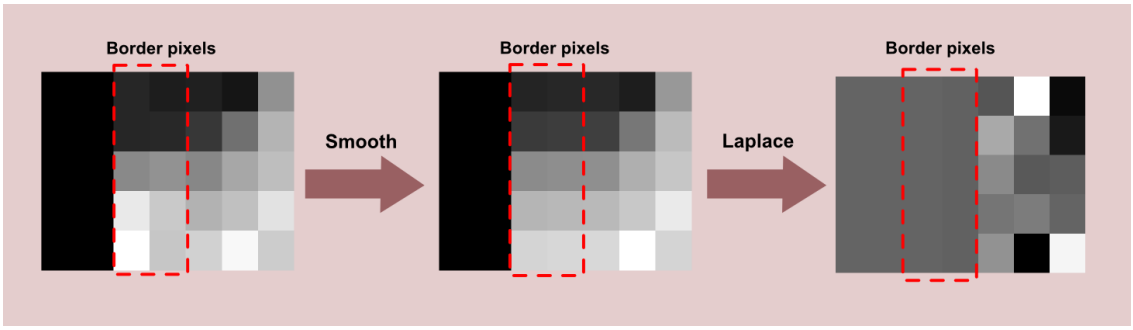

Figure 3. Illustration of smoothing two inner border pixels (in red-dashed box) in the truncated image in a row-wise. This results in a smoother transition after Laplace filtering and removal of the high spike.

Unlike 2D Laplace filter that uses a five-point stencil, 1D Laplace filtering is only performed in a row-wise and thus resulting values of each row are independent on its two adjacent rows. This would result in total different magnitude in the border pixels of the rows even they are neighbouring. The following residual filtering will amplify these differences and cause obvious streaking artifacts in the borders of filtered projections. To overcome this problem, an additional smoother is carried out only in the two inner pixels of truncated edge so that magnitudes of the border pixels are no significant difference after the Laplace operation, as shown in Figure 3.

2.4 Experiment Setup

The proposed algorithm was evaluated by the following data sets in terms of spatial resolution, computational efficiency and robustness of correction quality. All data sets contain 496 projection images (960×1240) with the resolution of 0.308 mm / pixel. Analogous to the 2D ATRACT algorithm, the new algorithm also suffers from a global volume scaling artifact. A correction of scaling and bias was performed to align the range of values between FDK and 1D ATRACT.

An open reconstruction benchmark (RabbitCT[17]) was employed to analyze the computational efficiency of the new algorithm. It is an open benchmark for comparison of reconstruction performance using a high resolution C-arm CT data set of a rabbit.

To evaluate the spatial resolution of the reconstructions with the new algorithm, we used projection images of the line-pair insert of the Siemens cone-beam phantom acquired on a C-arm system (Siemens AXIOM Artis). Two setups were considered: non-truncated projections and virtually cropped projections, as illustrated in Figure 4.

To quantify the robustness of the algorithm in presence of data truncation, we used a clinical data set acquired on a C-arm system (Siemens AXIOM Artis) from St. Lukes Episcopal Hospital. The patient is a 76 year old female with left ICA (Internal Carotid Artery) aneurysm treated with a pipeline stent. Two setups are exemplarily shown in Figure 5(a) and (b). We also investigated the performance of the 2D ATRACT method, and compared it to the new correction method.

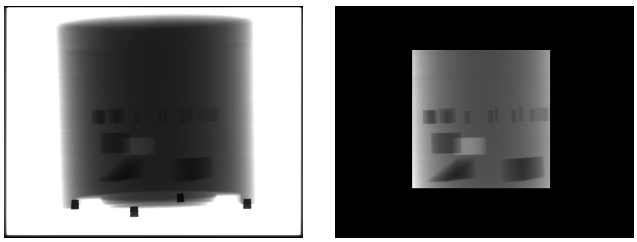

(a) (b)

Figure 4. Projection images of the Siemens cone-beam phantom. Two configurations were considered. (a) full FOV projection images (c) virtually collimated projection images.

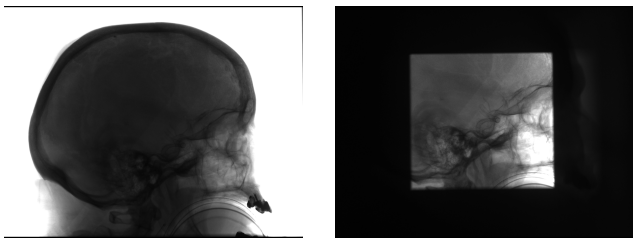

(a) (b)

Figure 5. Projection images of the clinical patient head data set. (a) Full FOV scan, DAP (Dose Area Product): $5667.4\ \mu\text{Gy}m^2$, (b) medium ROI scan, 30% of full FOV, DAP: $1630.9\ \mu\text{Gy}m^2$.

3. RESULTS

3.1 Computational Performance

As seen in Figure 6, 1D ATRACT is almost as fast as the ramp filter: Runtime is slightly increased by a factor of 1.1. Compared to the ramp filter, 1D ATRACT only has one addtional pre-filtering step, the Laplace filtering, which is computationally inexpensive. 2D ATRACT, on the other hand, is roughly 5.5 times slower than 1D ATRACT due to increased computational complexity and additional padding in 2D FFTs.

3.2 Spatial Resolution

Figure 7 shows the reconstructions of the line-pair phantom. The yellow arrows highlight the investigated line-pair insert that has a modulation of 1.8 lp / mm. The noise level of the given slices, estimated by computing the standard deviation within the yellow box, is 101.9 HU for the standard FDK reconstruction, and 103.6 HU for the 1D ATRACT reconstruction. The reconstruction results confirm that 1D ATRACT based ROI reconstruction yields, for the investigated insert, identical spatial resolution as the full FOV reconstruction by FDK. Note that 2D ATRACT was also demonstrated to yield the same spatial resolution as FDK.[14]

3.3 Correction Quality

The clinical patient head data set was reconstructed onto a Cartesian grid ($512 \times 512 \times 350$) with sampling spacing $\triangle x = \triangle y = \triangle z = 0.4$mm. The reconstruction results from transversal, sagittal and coronal planes are shown in Figure 8. It is clear that satisfying reconstruction results are obtained by the proposed method and 2D ATRACT. No bright

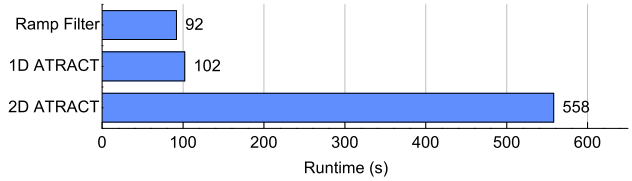

Figure 6. Runtimes of filtering of 496 projections (960×1240) in each algorithm. The results were computed in a single thread on an Intel ® Xeon X5570 CPU.

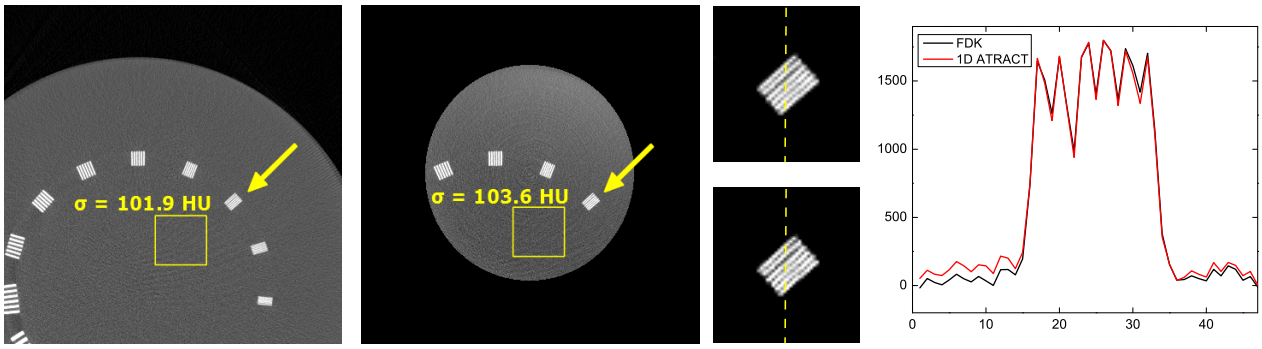

(a) (b) (c) (d)

Figure 7. Reconstruction results of the line-pair inserts phantom in the gray scale window [-500HU, 2000HU]. Slice thickness is 0.3mm. (a) Standard FDK reconstruction from non-truncated projections, (b) 1D ATRACT reconstruction from virtually truncated images, (c) zoomed view of the investigated line pair, (d) profiles along the yellow-dashed line.

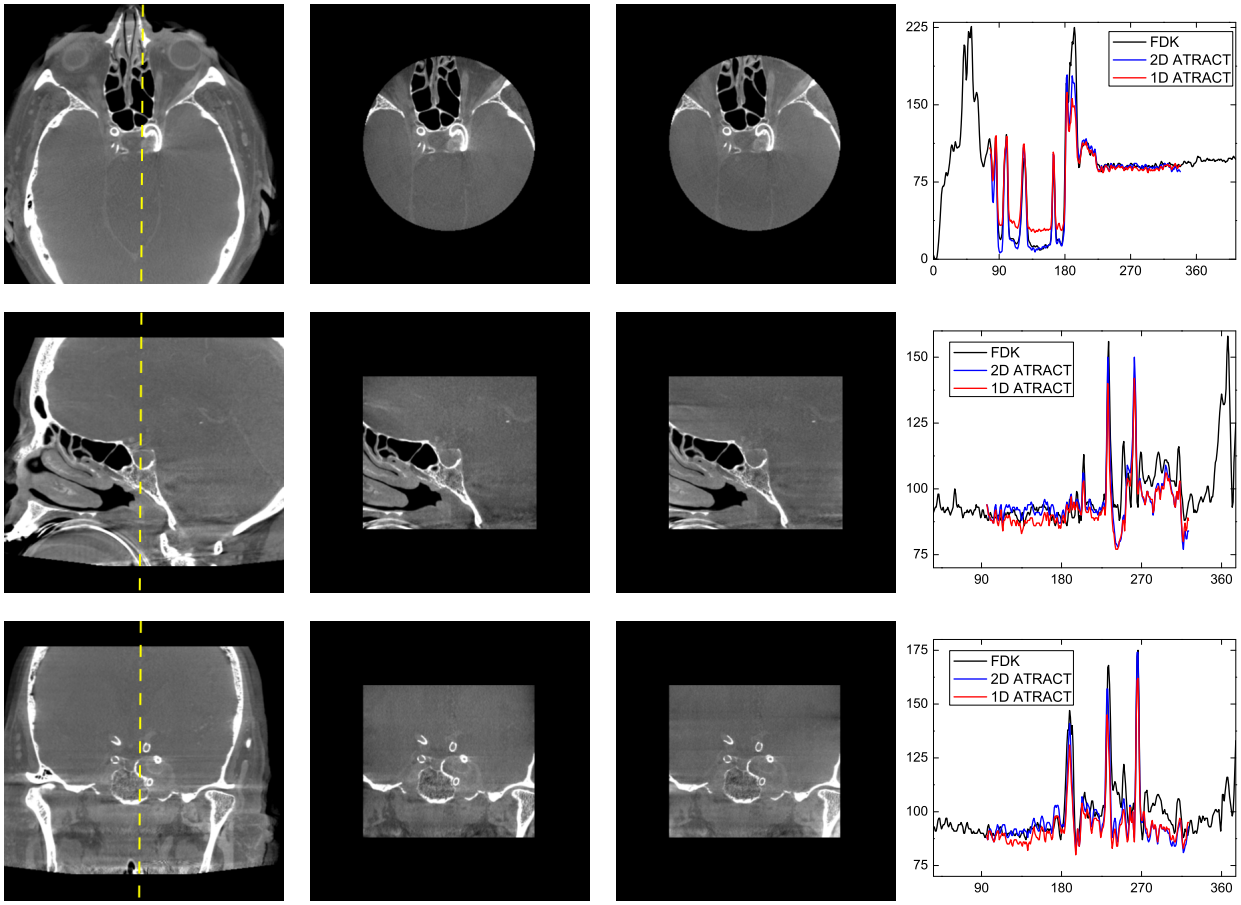

Figure 8. Multi-planar views of the reconstruction results of the clinical data set in the gray scale window [-500HU, 1000HU]. From left column to right column: FDK reconstruction from the full FOV scan (see Figure 5(a)), 2D ATRACT corrected reconstruction from the ROI scan (see Figure 5(b)), 1D ATRACT corrected reconstruction from the ROI scan, the reconstructed values (compressed) along the central profiles (dashed-yellow line) in each algorithm.

ring artifacts in the FOV are observed, which implies that high frequency artifacts are essentially suppressed by the two methods. At the same time, the portion of the patient inside the FOV are almost identical to the FDK reconstruction from full FOV scan. Further analysis is provided by the central profiles through the FOV of each reconstruction. Note that the differences between the FDK full FOV reconstruction and 1D/2D ATRACT based ROI reconstructions not only rely on the truncation artifacts, but also depend on the level of physical effects, such as X-ray scattering or polychromatic effects in the projections.

4. SUMMARY

In this paper, we presented a novel method that adapts the ATRACT method in one dimension by decomposing the standard ramp filter into the 1D Laplace filter and a 1D convolution-based filter. The corresponding convolution kernel was numerically estimated by computing the 1D impulse response of the standard ramp filtering coupled with the 1D inverse Laplace operation. The proposed algorithm showed the improvement in computational performance due to reduced computational complexity and less padding required in 1D FFTs with respect to the native ATRACT algorithm. Furthermore, reconstructions of high accuracy were maintained by the new method even in presence of data truncation.

ACKNOWLEDGMENTS

The authors gratefully acknowledge funding by Siemens AG, Healthcare Sector and of the Erlangen Graduate School in Advanced Optical Technologies (SAOT) by the German Research Foundation (DFG) in the framework of the German excellence initiative. All reconstruction results were computed with a Siemens prototype software, not a clinical product. The concepts and information in this paper were never submitted, published, or presented before.

REFERENCES

[1] Noo, F., Clackdoyle, R., and Pack, J. D., "A Two-step Hilbert Transform Method for 2D Image Reconstruction," *Physics in Medicine and Biology* **49**(17), 3903–3923 (2004).

[2] Pan, X., Zhou, Y., and Xia, D., "Image reconstruction in peripheral and central region-of-interest and data redundancy," *Medical Physics* **32**(3), 673–684 (2005).

[3] Defrise, M., Noo, F., Clackdoyle, R., and Kudo, H., "Truncated Hilbert transform and image reconstruction from limited tomographic data," *Inverse Problems* **22**(3), 1037–1053 (2006).

[4] Kudo, H., Courdurier, M., Noo, F., and Defrise, M., "Tiny a priori knowledge solves the interior problem in computed tomography," *Physics in Medicine and Biology* **52**(9), 2207 (2008).

[5] Chityala, R., Hoffmann, K. R., Bednarek, D. R., and Rudin, S., "Region of Interest (ROI) Computed Tomography," *Proceedings of Society Photo-Optical Instrumentation Engineers* **5368**(2), 534–541 (2004).

[6] Kolditz, D., Kyriakou, Y., and Kalender, W. A., "Volume-of-interest (VOI) imaging in C-arm flat-detector CT for high image quality at reduced dose," *Medical Physics* **37**(6), 2719–2730 (2010).

[7] Kolditz, D., Meyer, M., Kyriakou, Y., and Kalender, W. A., "Comparison of extended field-of-view reconstructions in C-arm flat-detector CT using patient size, shape or attenuation information," *Physics in Medicine and Biology* **56**(1), 39–56 (2011).

[8] Ohnesorge, B., Flohr, T., Schwarz, K., Heiken, J. P., and Bae, J. P., "Efficient correction for CT image artifacts caused by objects extending outside the scan field of view," *Medical Physics* **27**(1), 39–46 (2000).

[9] Hsieh, J., Chao, E., Thibault, J., Grekowicz, B., Horst, A., McOlash, S., and Myers, T. J., "A novel reconstruction algorithm to extend the CT scan field-of-view," *Medical Physics* **31**(9), 2385–2391 (2004).

[10] Maltz, J. D., Bose, S., Shukla, H. P., and Bani-Hashemi, A. R., "CT truncation artifact removal using water-equivalent thicknesses derived from truncated projection data," *IEEE Engineering in Medicine and Biology Society*, 2905–2911 (2007).

[11] Sourbelle, K., Kachelriess, M., and Kalender, W. A., "Reconstruction from truncated projections in CT using adaptive detruncation," *European Radiology* **15**(5), 1008–1014 (2005).

[12] Maier, A., Scholz, B., and Dennerlein, F., "Optimization-based Extrapolation for Truncation Correction," *2nd CT Meeting*, 390–394 (2012).

[13] Dennerlein, F., "Cone-beam ROI reconstruction using the Laplace operator," *Proceedings of Fully 3D 2011*, 80–83 (2011).

[14] Dennerlein, F. and Maier, A., "Region-of-interest reconstruction on medical C-arms with the ATRACT algorithm," *Proceedings of SPIE*, 83131B (2012).

[15] Xia, Y., Maier, A., Dennerlein, F., Hofmann, H. G., and Hornegger, J., "Efficient 2D filtering for cone-beam VOI reconstruction," *IEEE NSS-MIC*, 2415–2420 (2012).

[16] Feldkamp, L. A., Davis, L. C., and Kress, J. W., "Practical cone beam algorithm," *Optical Society of America* **1**(6), 612–619 (1984).

[17] Rohkohl, C., Keck, B., Hofmann, H. G., and Hornegger, J., "RabbitCT—an open platform for benchmarking 3D cone-beam reconstruction algorithms," *Medical Physics* **36**(9), 3940–3944 (2009).